Conclusions

A method for reducing propagated yaw estimation errors in a satellite attitude determination system with continuous roll and pitch measurements, but with yaw measurements available only for a portion of the orbit, is presented herein. The method relies on the coupling between roll and yaw that is inherent in the kinematics of an Earth-pointing satellite. When included in a Kalman filter formulation, this coupling acts to reduce the yaw estimation uncertainty during those periods when no yaw measurements are available. The continuous roll measurements, together with the orbital rate coupling, act indirectly to improve the estimate of the yaw attitude during these periods. An analytical method for predicting the rms error of the propagated yaw estimate is also presented, and is validated with simulation results.

References

[1]Lefferts, E. J., Markley, F. L., and Shuster, M. D., "Kalman Filtering for Spacecraft Attitude Estimation," *Journal of Guidance, Control, and Dynamics*, Vol. 5, No. 5, 1982, pp. 417–429.

[2]Sedlak, J., and Chu, D., "Kalman Filter Estimation of Attitude and Gyro Bias with the QUEST Observation Model," AAS Paper 93-297, Jan. 1993.

[3]Crassidis, J. L., Andrews, S. F., Markley, F. L., and Ha, K., "Contingency Designs for Attitude Determination of TRMM," *Proceedings of the Flight Mechanics/Estimation Theory Symposium*, NASA Goddard Space Flight Center, Greenbelt, MD, May 1995, pp. 419–433.

[4]Jayaraman, C. P., and Class, B., "On-Board Attitude Determination for the Explorer Platform Satellite," AAS Paper 91-484, Aug. 1991.

[5]Gelb, A., ed., *Applied Optimal Estimation*, MIT Press, Cambridge, MA, 1974, pp. 107–110, 119–121, 136, 137.

Strategy for Deployment of Multiple Satellites for Collision-Free Relative Orbital Motion

R. V. Ramanan*
Vikram Sarabhai Space Center, Thiruvananthapuram 695 022, India

Introduction

ORBITAL deployment of multiple satellites by a single vehicle is becoming increasingly important, with the emergence of low-Earth-orbit (LEO) satellite constellations for mobile communications and due to other factors such as reduced cost. To achieve the constellations, several satellites are put in orbit by a single launch vehicle. They are maneuvered afterwards to put them into the proper locations. Because these operations take many days or weeks, it is essential that the satellites remain in orbit without colliding with each other for several orbits.[1] Because these deployments are carried out with a separation system of springs, inducing very small changes among the bodies, the bodies move dangerously close, in approximately the same orbits. Also, when these deployments take place either simultaneously or in quick succession within shorter time intervals, the possibility of recontact between the separated bodies is real and of concern. The multiple satellite launch by India—PSLV-C2 or Polar Satellite Launch Vehicle-Continuation Flight 2 mission—required a deployment strategy to ensure noncollision between satellites. Spagnulo and Sabathier[2] discuss inclining the satellites in the stacking configuration and selecting the incremental separation velocities to increase the relative distance between the satellites. They arrive at these values by carrying out Monte Carlo (MC) analysis by propagating the orbits of the satellites with variations in the parameters involved in the deployment for various deployment strategies. This process of carrying out MC analysis is cumbersome and computationally demanding. A strategy based on simple orbit characteristics has been devised for the deployment of these satellites so that they will not collide in the long term (less than one synodic period of the satellites involved). The usage of this strategy avoids the necessity of carrying out MC analysis (repeatedly) to assess the collision possibility for different sets of deployment parameters.

Problem Description

Assume that from the last stage of a launch vehicle (parent body P), the satellite S_1 is separated at time t_1, and after a short interval of time Δt at t_2 (i.e., $\Delta t = t_2 - t_1$) another satellite S_2 is deployed. Because these deployments are carried out with a system of separation springs, they impart very small incremental velocities to the bodies. It is possible that satellite S_2 may collide with S_1, because they move in very close orbits. The possibility of collision exists only at the points that are common to both the orbits. If Δt is ignored (i.e., assuming that the satellites are released at the same time), the point from which the satellites are released is one such common point. If this is the only point, then collision is possible only at this point. Obviously, after separation, to come back to this point, the satellites have to complete one revolution. There may be more than one possible collision point depending on the geometry of the orbits. The existence of such common points is only a necessary condition for a collision possibility. The sufficient condition depends on the periods of revolution. Assume that the bodies are moving under the influence of a spherical central force field only.

If P_1 and P_2 are the periods of the orbits of S_1 and S_2, then collision will occur at the common points when $P_1 = nP_2$, where $n = l$ and $l = 1, 2, 3, \ldots$, and when $n = 1/k$, where $k = 1, 2, \ldots$. If the periods of the satellites are equal ($n = 1$), they will collide at the end of one revolution or before, depending on the geometry of the orbits. Also note that if the satellites do not collide within the first few orbits, the relative distance tends to grow with time. However, the two satellites separated with small incremental velocities would come closer after one synodic period even if they do not collide in the first few orbits. In this Note, a strategy to make the period of S_2 equal to that of S_1 so that they will collide after one revolution is presented with the mathematical model. Based on this, deployment of the satellites is carried out to ensure no collision in the long term and the procedure can be extended to other values of l and k.

Strategy for Collision

In the separation of satellites, two parameters, namely, the incremental velocity ΔV and its direction of application (referred to hereafter as orientation) described by the angle θ between V_P (instantaneous velocity vector of the parent body) and ΔV, determine the orbits of the satellites. Note that the incremental velocity is shared between the parent body ΔV_P and the satellite ΔV_S in accordance with

$$\Delta V_S = +|[m_2/(m_1+m_2)]\Delta V|, \qquad \Delta V_P = |[-m_1/(m_1+m_2)]\Delta V|$$

where m_1 and m_2 are masses of the parent body and the satellite. If ΔV_{S_1} and θ_1 and ΔV_{S_2} and θ_2 are the separation velocities and orientations of S_1 and S_2, respectively, then ΔV_{S_2} and θ_2 can be chosen so that the periods of orbits of S_1 and S_2 are equal.

Mathematical Model

Let the satellite S_1 be released with ΔV_{S_1} and θ_1 at t_1 and V_P be the velocity of the parent body before separation . Let P_1 be the period of revolution of S_1 after separation. The problem is to find ΔV_{S_2} and θ_2 for S_2 such that $P_1 = P_2$.

The period of the orbits of satellites is given by $P_i = 2\pi a_i^{3/2} / \sqrt{(\mu)}$ where $i = 1, 2$ and $a_i\{i = 1, 2\}$ are the semimajor axes and μ is gravitational constant.

Received 5 April 1999; revision received 15 November 1999; accepted for publication 15 December 1999.

*Scientist, Astronautics and Orbital Mechanics, Applied Mathematics Division.

To make the periods equal, the semimajor axes must be equal. The semimajor axes a_1 and a_2 are related to the velocities V_{S_1} and V_{S_2} at t_2 by the vis-viva equation[3]

$$V_{S_i}^2 = \mu(2/r_i - 1/a_i), \qquad i = 1, 2$$

at t_2. Under the assumption that Δt is ignored and the satellites are released at the same time, we get $r_1(t_2) = r_2(t_2)$ implying that ΔV_{S_2} and θ_2 must be chosen such that $V_{S_1}(t_2) = V_{S_2}(t_2)$ to make $a_1 = a_2$ and, hence, $P_1 = P_2$.

Now it remains to relate the separation velocity, orientation ΔV_{S_2} and θ_2, and the resultant velocity $V_{S_2}(t_2)$. The relation by the law of cosines

$$V_{S_2}^2(t_2) = V_P^2(t_2) + \Delta V_{S_2}^2(t_2) - 2\Delta V_{S_2}(t_2)V_P(t_2)\cos(\theta_2) \qquad (1)$$

satisfies this requirement.

Because for the periods P_1 and P_2 to be equal, ΔV_{S_2} and θ_2 have to be chosen such that $V_{S_1}^2(t_2) = V_{S_2}^2(t_2)$, Eq. (1) is rewritten as,

$$V_{S_2}^2(t_2) = V_{S_1}^2(t_2) = V_P^2(t_2) + \Delta V_{S_2}^2 - 2\Delta V_{S_2} V_P(t_2)\cos(\theta_2) \qquad (2)$$

In Eq. (2), because $V_{S_1}(t_2)$ and $V_P(t_2)$ are known quantities by propagation of S_1 and the parent body P until $t = t_2$, various combinations of ΔV_{S_2} and θ_2 can be obtained resulting in $P_1 = P_2$.

For a given orientation θ_2, the magnitude of separation velocity ΔV_{S_2}, making P_1 equal to P_2 and, hence, leading to collision of S_1 and S_2, is given by the solution of the quadratic equation in ΔV_{S_2},

$$\Delta V_{S_2}^2 - 2V_P\cos(\theta_2)\Delta V_{S_2} + \left[V_P^2 - V_{S_1}^2\right] = 0 \qquad (3)$$

For a given ΔV_{S_2}, the orientation θ_2 making P_1 equal to P_2 and, hence, leading to collision of S_1 and S_2 is given by

$$\cos(\theta_2) = \frac{V_P^2(t_2) - V_{S_1}^2(t_2) + \Delta V_{S_2}^2}{2\Delta V_{S_2}(t_2)V_P(t_2)} \qquad (4)$$

Deployment Strategy for Noncollision

The noncollision deployment strategy, which is deduced from the strategy for collision and which will be useful for mission analysts, is described in this section. Using Eqs. (3) or (4), a plot can be drawn for ΔV_{S_2} vs θ_2 or θ_2 vs ΔV_{S_2}. If ΔV_{S_2} and the range $[\Delta V_{\min}, \Delta V_{\max}]$ in which it varies are known, then from the plot, θ_2 can be chosen so that any ΔV_{S_2} in $[\Delta V_{\min}, \Delta V_{\max}]$ will not lead to collision with θ_2 being the orientation. Likewise, if the orientation θ_2 and its range $[\theta_{\min}, \theta_{\max}]$ are known, then from the plot ΔV_{S_2} is chosen such that it will not constitute a collision combination with any value $\theta_2 \in [\theta_{\min}, \theta_{\max}]$. This analysis can be extended to include θ_2 variation in the first case and ΔV_{S_2} variation in the second case. Also, the strategy can be extended to include variations in ΔV_{S_1} and θ_1.

Illustrative Example and Numerical Results

Although the strategy developed is based on the assumption that the satellites are released simultaneously, it is also applicable for satellites released with a small time gap so long as the difference in radial distances are reasonably small. This is demonstrated in the following. When $\Delta t \neq 0$, the values of V_P and V_{S_1} are found at $t = t_2$ by propagation of the orbits of P and S_1 until $t = t_2$ from $t = t_1$ and substituted in Eq. (4). For orbit propagation only a Kepler force model is used.

Two satellites, S_1 and S_2, deployed by a parent body P are considered. The sequence is t_0 = thrust cutoff, $t_1 = t_0 + 27$ s (S_1 separation), and $t_2 = t_1 + \Delta t$ (S_2 separation). The orbital elements of P at t_0 are semimajor axis = 7100.605 km, eccentricity = 0.000023495, inclination = 98.377 deg, right ascension of ascending node = 184.657 deg, argument of perigee = 26.349 deg, mean anomaly = 169.8106 deg, and period = 5954.619 s.

The separation velocity and its nominal orientation are given in Table 1. S_1 is separated with 0.8071 m/s relative velocity with $\theta_1 = 14.26$ deg. S_2 is separated with 1.0014 m/s relative velocity. The problem now is to determine θ_2 for S_2 separation that leads to collision with S_1 for various values of Δt.

The combination for S_1-S_2 close contact using the strategy presented is found to be (0.9049 m/s, −30.182926 deg) for $\Delta t = 0$ s and (0.9049 m/s, −30.455951 deg) for $\Delta t = 50$ s, referred to as the collision combinations. The propagation of the orbits of S_1 and S_2 after separation confirms this conclusion. Because the collision angle is with respect to the body-centered frame, a transformation[4] is effected to obtain incremental velocity components in the geocentric inertial frame before carrying out the propagation. The separation of S_2, 50 s after S_1 separation, with 1.0014 m/s relative velocity (0.9049 m/s separation velocity for S_2) after orienting the vehicle by −30.455951 deg results in a very close approach of S_1-S_2 with only 85 cm being the relative distance after nearly one revolution (T_2 + 5940 s) . Also, if S_1 and S_2 are separated simultaneously, an orientation of −30.182926 deg leads to a minimum relative distance of 26 cm after one revolution (T_2 + 5956 s). Clearly these results confirm the performance of the strategy.

Table 1 Velocity shares and directions

Time, s	Event	Body (mass)	ΔV_S, m/s Imparted	Orientation θ, deg
T_1	S_1	$P + S_2$ (1141 kg)	0.3868 ΔV_P	194.26
	Separation	S_1 (1050 kg)	0.4203 ΔV_{S_1}	14.26
T_2	S_2	P (1031 kg)	0.0965 ΔV_P	Unknown
	Separation	S_2 (110 kg)	0.9049 ΔV_{S_2}	Unknown

In addition to the data provided for $\Delta t = 0$ and 50 s, several more sets of results are provided (Δt, orientation angle, minimum relative distance, and time of occurence): (5 s, −30.185666 deg, 3.522 m, T_2 + 5954 s), (10 s, −30.193889 deg, 6.273 m, T_2 + 5953 s), (20 s, −30.226764 deg, 9.423 m, T_2 + 5950 s), (30 s, −30.281482 deg, 9.459 m, T_2 + 5946 s), (40 s, −30.357930 deg, 6.390 m, T_2 + 5943 s), (60 s, −30.575348 deg, 9.248 m, T_2 + 5937 s), (70 s, −30.715882 deg, 21.684 m, T_2 + 5934 s), (80 s, −30.877278 deg, 37.259 m, T_2 + 5931 s), (90 s, −30.059225 deg, 55.963 m, T_2 + 5928 s), and (100 s, −30.261382 deg, 77.794 m, T_2 + 5925 s). When Δt increases, the accuracy of prediction of separation conditions using the strategy suffers. This is because $r_1 \neq r_2$ when $\Delta t \neq 0$ and two angles (in-plane and out-of-plane) are required to specify the direction of ΔV. Still, this strategy gives an idea about the region of separation conditions with which collision is likely to occur when Δt is larger. The exact collision between satellites takes place in the neighborhood of the orientation angles just indicated. The force models 1) Kepler, 2) Kepler plus Goddard Earth Model (GEM)T1, and 3) Kepler + drag are considered to study the effect of nonspherical gravity field and drag on the solution obtained through the strategy for $\Delta t = 50$ s. For drag computations, the following values are used: $C_D = 2.2$, area of $S_1 = 12.2$ m^2, area of $S_2 = 0.665$ m^2, $F_{10.7} = 150.0$, and $A_P = 4.0$. For the three force models, the orientation, the minimum relative distance, and its time of occurrence are (−30.455972 deg, 0.851 m, T_2 + 5940 s), (−30.456138 deg, 2.532 m, T_2 + 5946 s), (−30.455972 deg, 0.937 m, T_2 + 5940 s). The effects of perturbing accelerations on the satellites are not distinctly different and nullify each other for the first few orbits, and, hence, the relative motion of the satellites is unaffected. The strategy could produce separation conditions ΔV_{S_2} and θ_2, leading to S_1-S_2 collision independent of the force model. Though the orbit considered in the example problem is nearly circular, the strategy produces a nearly exact solution even when the orbits are elliptic; however, those results are not included here.

The next task is to find the separation velocity of S_2 (ΔV_{S_2}) and the orientation of $S_2(\theta_2)$ avoiding a close-contact possibility between S_1 and S_2. Figure 1 is drawn using Eq. (4). It is inferred that any separation velocity for S_2 deployment less than 0.78 m/s will completely avoid an S_1-S_2 close-contact possibility for all orientations. This conclusion is made on the assumption that the S_1 separation is nominal, and similar conclusions can be drawn including deviations in the performance of S_1 separation. Also if S_2 is separated with 1.0014 m/s relative velocity and if ΔV_{S_2} can vary in [0.85 m/s, 0.95 m/s], the orientation has to be such that θ_2 lies in

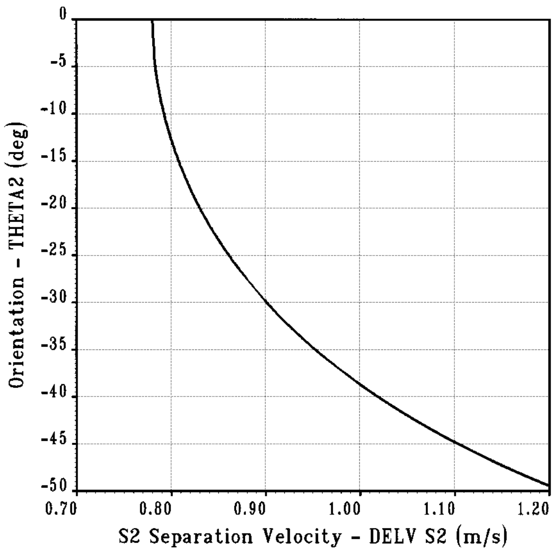

Fig. 1 Separation conditions of S_2 for collision with S_1.

the range (−23.0 deg, 23.0 deg) or $|\theta_2| > 35$ deg to avoid an S_1-S_2 close-contact possibility. Note again that arriving at these conclusions through MC analysis is computationally demanding and time consuming because many combinations have to be tried in which a large number of simulations (orbit propagation) for each of the combinations is carried out.

Although the strategy is demonstrated in the case of two satellites, it can be used[5] even when there are more satellites to find deployment conditions for each satellite to avoid a close-contact possibility among all of them. A system of separation springs for satellites can be designed to meet the noncollision separation velocity taking into account the masses. Also, orientation can be planned through proper control strategies. The orientation angle leading to recontact of P and S_1 and P and S_2 can also be computed using this strategy. For this example, no angle leads to such a recontact possibility between P and S_1 and an angle of approximately 90 deg leads to the collision of P and S_2.

Conclusions

A strategy to arrive at separation velocity and its orientation with respect to instantaneous velocity, for the deployment of a satellite such that it avoids collision with another satellite in orbit within one revolution, deployed either simultaneously or a short time earlier, has been presented. Efficiency of the strategy under various force models and variations in the time gap between the deployments of the satellites has been analyzed. This strategy enables postinjection operations on satellites to put them into the proper location without the risk of collision. The fuel onboard, generally carried to account for collision risk, can be saved.

Acknowledgments

The author expresses his sincere thanks to reviewers for their comments and observations. He wishes to express his gratitude to V. Adimurthy, Shri Madanlal, Shri K. Kumar, and P. V. Subba Rao, for their encouragement and for technical discussions.

References

[1] Yarbrough, P. G., "Operation Concept for the World's First Commercially Licensed Low-Earth Orbiting Mobile Satellite Service," AIAA Paper 96-1049-CP, Feb. 1996.

[2] Spagnulo, M., and Sabathier, V., "An Ariane Strategy for In-Orbit Separation of Satellite Constellations," *Proceedings of the 46th International Astronautical Congress*, International Astronautical Federation, IAF-95-A.6.06, 1995.

[3] Brown, C. D., *Spacecraft Mission Design*, AIAA Education Series, AIAA, Washington, DC, 1992, p. 14.

[4] Escobal, P. R., *Methods of Orbit Determination*, Wiley, New York, 1965, p. 397.

[5] Ramanan, R. V., "On the Collision Possibility of Satellites Deployed by a Single Vehicle During First Revolution," VSSC-APMD-TM-PSLV-017-1998.

Minimization of Vibration of Spacecraft Appendages During Shape Control Using Smart Structures

Serdar Kalaycioglu* and David Silva†
Canadian Space Agency,
St. Hubert, Quebec J3Y 8Y9, Canada

I. Introduction

LARGE space structures are inherently flexible, and this property tends to slow down, while increasing the cost of critical space maneuvers such as space station remote manipulator system positioning, and the deployment and orientation of solar panels, antennas, etc. The advent of smart structures is perceived as a promising alternative for the implementation of improved sensing and active control of vibration and shape for the next generation of large flexible space structures, such as space stations. Although there exist many alternatives to develop smart structures that can be used to implement the different modern shape control approaches, we concentrate on the use of PZTs. The modeling of the induced-strain actuation produced by these devices can be found in the work of Crawley and Anderson.[1]

In this Note, a dynamic model, originally developed in a flexible appendage deployment context,[2] is extended to include a smart structure and is used to minimize the vibrational motion of an elastic cantilevered plate with a glued collocated sensor/actuator pair of fiber-optic strain sensor and piezoceramic actuator (PZT), during the application of a static shape control scheme.

The process of shape control based on smart structures estimates the target voltage values for the PZT actuators to correct the deformed shape of an appendage. However, the voltage profiles, that is, variation of voltage with respect to time, for each actuator may not be obtained because the shape control process provides only the initial and final static voltage values. After direct application of these voltages, via the PZT actuators, a successful shape correction of the appendage can be realized. Nevertheless, the arbitrary selection of any admissible control voltage profile leading from the initial voltage values to the final voltage values causes transient and residual vibrations.

The optimum voltage profile is obtained using Pontryagin's principle for the variation of the PZT voltages, under the restriction of minimum vibrational motion during the shape correction process. The resulting two-point boundary problem is solved using a multiple-shooting algorithm to obtain the desired optimum solution. The optimum solution is exhibited, experimentally tested, and compared with other admissible control profiles.

II. Dynamic Model of the Smart Structure

The flexible appendage of a spacecraft is characterized by means of a plate with some glued or embedded piezoceramic actuators and fiber-optic strain sensors. An example of the geometry of such a system is shown in Fig. 1.

In Fig. 1, A_0, B_0, and H_0 represent the physical dimensions of the plate, whereas A_i, B_i, and H_i are those of the PZT actuators, with $i = 1, \ldots, m$, where m is the number of actuators. In Fig. 1, the coordinate axes are represented by x, y, and z.

Let the instantaneous transverse elastic displacement along the z axis be $w(x, y, t)$. For the convenience of the analysis we assume that w is separable into its temporal and spatial components, and

Received 15 May 1997; revision received 14 September 1999; accepted for publication 8 November 1999.

*Manager, Strategic Automation and Robotics Technologies, 6767 Airport Road; serdar.kalaycioglu@space.gc.ca.

†Student Employee, Space Technologies Branch; currently Engineer, CAE Electronics, 8585 Cote de Liesse, Saint-Laurent, Quebec, Canada H4T 1G6.